

Motor and Sensory Function-based Ensemble Learning Classifiers for Detecting Cognitive Decline Subtypes

Shinyoung Lee,^{1†} Kiyoun Kwak,^{2†} Emilija Kostic,¹ and Dongwook Kim^{2,3*}

¹Department of Healthcare Engineering, The Graduate School, Jeonbuk National University,
567 Baekje-daero, Deokjin-gu, Jeonju-si, Jeollabuk-do 54896, Republic of Korea

²Division of Biomedical Engineering, College of Engineering, Jeonbuk National University,
567 Baekje-daero, Deokjin-gu, Jeonju-si, Jeollabuk-do 54896, Republic of Korea

³Research Center for Healthcare & Welfare Instrument for the Elderly, Jeonbuk National University,
567 Baekje-daero, Deokjin-gu, Jeonju-si, Jeollabuk-do 54896, Republic of Korea

(Received October 8, 2024; accepted June 11, 2025)

Keywords: mild cognitive impairment (MCI) subtypes, machine learning, motor function, sensory function, classification

Mild cognitive impairment (MCI) is the transitional stage between cognitively healthy aging and dementia, characterized by subtle neurocognitive changes, and can be categorized into two variants: amnesic and non-amnesic. These subtypes have different progressions and incidences of dementia, making detection challenging. On the basis of evidence from previous studies that investigated the motor and sensory functions in different MCI subtypes, we hypothesized that motor and sensory function variables can be used to develop a cost-effective classification tool that can distinguish cognitive decline subtypes. Community-dwelling men ($N = 117$) over 65 participated in this study. We assessed the participants' motor-sensory function and developed classification models for dividing them into cognitive decline subtypes. In this study, we developed Random Forest (RF), Gradient Boosting, XGBoost, and Histogram-based Gradient Boosting models. RF was the most effective, with an accuracy of 0.833, an area under the curve 95% confidence interval ranging from 0.965 to 0.978, a specificity ranging from 0.835 to 0.988, and a sensitivity ranging from 0.469 to 0.932. Both the sensitivity and specificity for detecting non-memory-related cognitive decline were high; therefore, the motor and sensory function-based classification models developed in this study are anticipated to aid in the diagnosis of MCI subtypes, especially non-amnesic MCI.

1. Introduction

With the aging of the global population, cognitive decline, particularly mild cognitive impairment (MCI), has emerged as a critical public health issue.⁽¹⁾ MCI represents an intermediate stage between normal aging and dementia, characterized by a decline in cognitive function that does not meet the criteria for dementia diagnosis.⁽²⁾ Approximately 10–15% of individuals with MCI progress to dementia annually.⁽³⁾ The prevalence of MCI is reported to

*Corresponding author: e-mail: biomed@jbnu.ac.kr

[†]Sinyoung Lee and Kiyoun Kwak contributed equally to this work as co-first authors.

<https://doi.org/10.18494/SAM5631>

range between 10 and 20% among the elderly, and as it continues to rise, MCI is becoming a major issue in aging societies.⁽⁴⁾

It has been shown that MCI can be maintained or reversed with proper management, leading to an increased interest in the early diagnosis of MCI.⁽⁵⁾ Yaffe *et al.* emphasized that the subtype of MCI significantly affects the subsequent type of dementia,⁽⁶⁾ highlighting the critical role that the early diagnosis and management of MCI play in dementia prevention.

MCI is classified into amnesic (aMCI) and non-amnesic (naMCI) types on the basis of the presence of memory impairment. In aMCI, memory decline is the predominant symptom, which significantly increases the likelihood of progression to Alzheimer's disease (AD), with approximately 20% of aMCI patients progressing to AD.⁽⁷⁾ In contrast, naMCI is characterized by cognitive decline in non-memory domains, posing a higher risk of progression to frontotemporal dementia or Lewy body dementia.⁽⁸⁾ Studies highlighting distinct cognitive function differences between these subtypes indicate that distinguishing MCI subtypes may aid in understanding the progression of each dementia type and in developing tailored treatment strategies.⁽⁹⁾

For the above reasons, various prior studies have classified MCI subtypes using different approaches.^(10–12) The primary methods employed include neuropsychological evaluations, radiological analyses (e.g., magnetic resonance imaging (MRI) and positron emission tomography (PET)), and biological marker analyses (e.g., apolipoprotein E (APOE) genotype). However, these methods (1) are costly, (2) are affected by psychological conditions such as depression or anxiety,⁽¹³⁾ and (3) require advanced technology and expertise.⁽¹⁴⁾ In addition, biological markers can differ significantly between individuals, which poses a challenge in accurately detecting dementia subtypes.⁽¹⁵⁾

As an alternative solution, diagnostic methods based on motor and sensory functions can be used. Motor and sensory dysfunctions often precede the cognitive symptoms shown in Alzheimer's disease and can be identified during the MCI stage.⁽¹⁶⁾ Previous studies indicate that gait variability is significantly higher in aMCI than in naMCI,⁽¹⁷⁾ which contributes to the increased risk of falls.⁽¹⁸⁾ Therefore, a deterioration in motor function is more likely to be observed in aMCI. Visual function is associated with the parietal lobe, a cerebral region primarily linked to naMCI, which is essential for visual attention and visuospatial processing.^(19,20) Accordingly, visual impairments may be more prevalent in naMCI. On the other hand, auditory function is predominantly regulated by the temporal lobe,⁽²¹⁾ which deteriorates more in the case of aMCI,⁽²²⁾ making auditory decline a more likely symptom in aMCI.

Considering the association of motor and sensory functions with various cognitive domains,^(23,24) we expect the classification models to correctly classify individuals with cognitive decline into subtypes based on the motor and sensory characteristics. Therefore, in this study, we explored the potential of using easily measurable motor and sensory function biomarkers to achieve the early diagnosis of cognitive decline subtypes.

2. Methods

2.1 Participants

One hundred and seventeen community-dwelling men aged over 65 participated in this study. The study participants were able to walk without any assistance and had no history of serious neurological or musculoskeletal diseases. Cognitive, motor, and sensory functions were measured in two visits, one week apart. At the first visit, the participants underwent cognitive function tests and level walking assessments. After that, balance, visual, and auditory functions were measured at the second visit. All participants signed a written informed consent form after receiving detailed explanations about the study's purpose, content, and methods. In addition to the cognitive, motor, and sensory data, demographic information (age, height, weight, and years of education) was collected and used in the analysis. This study was approved by the Institutional Review Board of Jeonbuk National University (JBNU IRB File No.2022-04-017-003).

2.2 Cognitive function test

The Montreal Cognitive Assessment (K-MoCA) (Korean version) was performed to determine the participants' cognitive function, and the K-MoCA overall score and the memory index score (MIS) were used to classify them into three groups. According to the criteria, participants with less than 12 years of education had 1 point added to their K-MoCA score.⁽²⁵⁾ Participants with a K-MoCA score of 26 or higher were classified as the normal cognition (NC) group. Utilizing MIS to more accurately distinguish amnesic cognitive decline, we classified those with a K-MoCA score <26 and $MIS \geq 8$ as the normal-memory index score (N-MIS) group, whereas those with a K-MoCA score <26 and $MIS < 8$ were classified as the lower-memory index score (L-MIS) group.⁽²⁶⁾

2.3 Level walking and balance function measurement

To measure level walking, 17 infrared-emitting diodes (Smart marker, Northern Digital Inc., Canada) were attached to the lower body of the participants. Participants walked across four force plates (4060-08, Bertec Co., Ltd., USA) installed between three 3D position sensors (Optotrak Certus, Northern Digital Inc., Canada) arranged to face each other. They walked at a preferred pace for approximately 10 m, and the three-trial average of the spatiotemporal variables was calculated using the 3D musculoskeletal analysis software SIMM (Muscular Graphics, Inc., USA). The quantitative walking variables, cadence, and velocity, which were reported as indicators of cognitive decline⁽²⁷⁾ and are associated with the neuropathology of Alzheimer's dementia,⁽²⁸⁾ were used in the analysis.

Balance function was assessed using the tandem Romberg test under two conditions: eyes open and eyes closed. This test evaluates the ability to maintain balance while the feet stay in a heel-to-toe position. Participants were instructed to place one foot in front of the other, cross their arms over their chest, and rest them on their shoulders. Participants were asked to maintain

the stance for a maximum of 60 s per trial. When the participants lost balance or could not maintain the position, the measurement was halted early. The duration of posture maintenance under each condition was used as a variable for analysis. Descriptions of the balance, visual, and auditory function variables are presented in Table 1.

2.4 Visual and auditory function measurement

Visual acuity (VA) was measured using Jin's vision chart. For the participants wearing myopia glasses, the uncorrected visual acuity without glasses was measured first, followed by the corrected visual acuity measurements. The corrected and uncorrected visual acuities for each eye were measured and the averages were used as a variable. In addition, a variable investigating whether participants wear glasses was included in the analysis.

The Korean speech auditory test and audiometer (GSI-61, Grason-Stadler, Denmark) were used to measure hearing function in a soundproof room using prerecorded examples. Pure tone audiometry (PTA) and speech recognition threshold (SRT) were assessed. The average PTA thresholds of three frequency bands, namely, low (125, 250, and 500 Hz), normal speech (500, 1000, and 2000 Hz), and high (4000, 6000, and 8000 Hz), were used in the analysis. For both PTA and SRT, the better threshold of the two ears was used as the variable. Descriptions of visual and auditory function variables can be found in Table 1.

2.5 Ensemble learning process

Ensemble learning is an appropriate tool for analyzing complex and heterogeneous data and has the potential to reveal patterns and relationships that existing statistical techniques can overlook.⁽²⁹⁾ In the medical field, machine learning has contributed to improving the quality of patient treatment by providing personalized diagnosis, the increased accuracy of medical image analysis, and improved diagnostic efficiency.^(30–33)

In this study, ensemble learning algorithms were utilized to classify cognitive decline subtypes on the basis of demographic information, gait, balance, and sensory function variables. The entire process of model development and evaluation was conducted using PyCharm

Table 1
Descriptions of balance, visual, and auditory function variables.

Variable	Description
RT_EO	Maintenance time of tandem Romberg test when eyes are opened
RT_EC	Maintenance time of tandem Romberg test when eyes are closed
VA_un_avg	Average of right and left uncorrected visual acuities
BCVA	Average of right and left corrected visual acuities (For participants who are not wearing glasses, BCVA is the same as VA_un_avg.)
Glasses	Whether participants wear myopia glasses (0 – no, 1 – yes)
PTA_B	Better result of PTA at 500, 1000, and 2000 Hz
PTA468_B	Better result of PTA at 4000, 6000, and 8000 Hz
PTA125_B	Better result of PTA at 125, 250, and 500 Hz
SRT_B	Better result of SRT

Community Edition 2024.1.4 (JetBrains, Ltd., Czechia). Several Python packages, including NumPy, Pandas, Matplotlib, Scikit-learn, Imbalanced-learn, and SciPy, were employed. The ensemble learning workflow is illustrated in Fig. 1.

2.5.1 Data collection and processing

In this study, 198 data samples were collected from 117 participants. The data collection was structured as follows: 81 participants took part in the measurement experiments twice, one year apart, resulting in 162 samples, whereas 36 participants completed one experiment each, resulting in 36 samples. Data consisted of demographics (age, height, weight, and years of education), motor function variables (gait and balance), and sensory function variables (vision and hearing). These variables served as input data for ensemble learning classification models. The objective was to classify the participants into three types: NC, N-MIS, and L-MIS.

Because ensemble learning models are sensitive to the scale of variables, the data was scaled and then used to develop a classification model. Z-score normalization was applied so that the mean of all data values was 0 and the standard deviation was 1.⁽³⁴⁾

2.5.2 Feature selection

SelectKBest, a feature selection method provided by the Scikit-learn library, ranks variables on the basis of ANOVA F-statistics and selects the top K variables with the highest scores.⁽³⁵⁾ In this study, K was determined by considering the sample-to-variable ratio, a critical factor in ensuring robust model performance. A sample-to-variable ratio of at least 15–20 observations per independent variable is recommended to ensure sufficient data for the accurate evaluation of variable impact.⁽³⁶⁾ Therefore, in this study, K was set to 10 because the number of samples was 198.

2.5.3 Ensemble learning models

Classification models based on random forest (RF), gradient boosting (GB), XGBoost (XGB), and histogram-based GB (HGB) algorithms were developed using the Scikit-learn package. The aforementioned models utilize ensemble learning methods, which effectively combine several

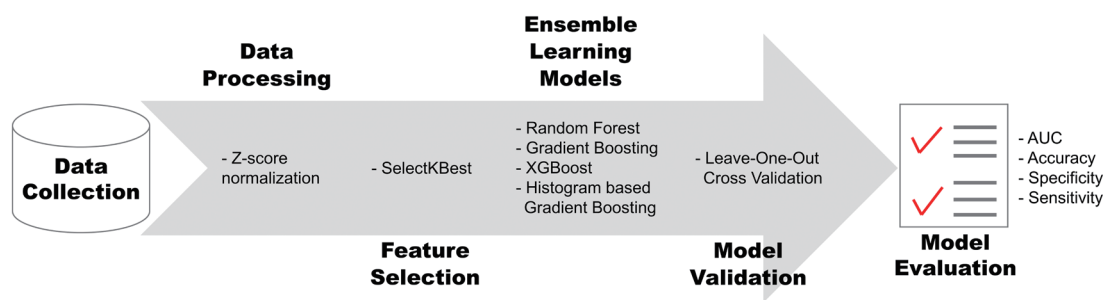


Fig. 1. (Color online) Overview of ensemble learning workflow.

individual models to build a better-performing model. Ensemble learning methods are particularly adept at discovering complex patterns within heterogeneous datasets by aggregating predictions across different models, thus reducing both bias and variance.⁽³⁷⁾ Furthermore, by mitigating individual biases, these methods help to reduce overfitting, particularly in cases of small datasets.⁽³⁸⁾ RF, which uses a bagging method, has good classification performance on small datasets by reducing variance through the aggregation of many decision tree classification results and by emphasizing general patterns over specific noise.⁽³⁹⁾ Boosting methods are particularly advantageous for classification tasks involving imbalanced classes, as they iteratively focus on correcting errors in previously misclassified samples, ensuring that minority classes are not overlooked.⁽⁴⁰⁾

2.5.4 Model validation

The model was validated using leave-one-out cross-validation (LOOCV). In this method, each data point is used once as a test set while the remaining data points are organized into a training set. This method enhances the model's generalization capacity by preventing overfitting to specific data samples, which is especially useful for small datasets.⁽⁴¹⁾

2.5.5 Model evaluation

The receiver operating character (ROC) curve is a representative assessment method of model performance. The area under the curve (AUC) was calculated to evaluate the model's classification performance. Sensitivity and specificity were computed to investigate its clinical utility.⁽⁴²⁾ The AUC value ranges from 0 to 1. The closer it is to 1, the better the classification performance. If the AUC value is 0.5, the model is performing random prediction. An AUC value ranging from 0.5 to 0.7 signifies that the model's classification performance is poor, an AUC value from 0.7 to 0.9 denotes good performance, and an AUC value above 0.9 means excellent performance.⁽⁴³⁾

3. Results

3.1 Functional characteristics of groups

The results of participants' cognitive function test and independent variables used in the ensemble models are presented in Table 2.

Of the 198 data samples, 88 were classified as NC, 78 as N-MIS, and 32 as L-MIS. Both K-MoCA and MoCA-MIS scored highest in the order of NC, N-MIS, and L-MIS groups.

The SelectKBest algorithm was employed to select variables, and the chosen variables were Age, YearsEducation, Cadence, Velocity, RT_EC, RT_EO, PTA_B, PTA468_B, PTA125_B, and SRT_B. The average age of the study participants was found to be the lowest in the NC group and the highest in the L-MIS group. In contrast, the number of years of education was the lowest in L-MIS and the highest in NC. For gait-related variables, both cadence and velocity were the

Table 2

Cognitive, demographic, gait, balance, and sensory function characteristics of each group.

		NC (Num = 88)	N-MIS (Num = 78)	L-MIS (Num = 32)
Cognitive variables	K-MoCA (pts)	27.38 ± 1.23	23.65 ± 1.35	22.13 ± 2.15
	MoCA-MIS (pts)	12.89 ± 2.18	10.86 ± 1.79	5.41 ± 1.68
	Age (years)	74.59 ± 3.83	76.32 ± 3.36	77.69 ± 4.39
Independent variables	YearsEducation (years)	14.35 ± 3.17	13.05 ± 3.58	12.53 ± 4.64
	Height (cm)	165.53 ± 6.16	166.06 ± 5.71	166.97 ± 6.68
	Weight (kg)	66.24 ± 7.17	67.00 ± 7.75	66.75 ± 8.46
	Cadence (spm)	113.40 ± 8.26	112.06 ± 6.81	108.64 ± 8.89
	Velocity (cm/s)	123.43 ± 16.71	117.41 ± 17.36	111.65 ± 18.22
	RT_EC (s)	9.84 ± 13.94	6.44 ± 8.49	5.94 ± 10.02
	RT_EO (s)	43.36 ± 22.43	37.74 ± 24.89	31.00 ± 25.70
	VA_un_avg	0.68 ± 0.28	0.66 ± 0.27	0.65 ± 0.24
	BCVA	0.77 ± 0.24	0.75 ± 0.25	0.74 ± 0.28
	Glasses (num)	29	20	10
	PTA_B (dBHL)	19.67 ± 10.26	22.24 ± 9.46	23.54 ± 10.62
	PTA468_B (dBHL)	53.22 ± 14.78	58.80 ± 13.16	58.44 ± 15.19
	PTA125_B (dBHL)	15.00 ± 9.82	17.44 ± 9.47	22.14 ± 12.09
	SRT_B (dBHL)	17.73 ± 10.6	19.42 ± 9.70	21.56 ± 11.53

Mean ± SD, NC: normal cognitive, N-MIS: normal-memory index score, L-MIS: lower-memory index score, Num: number of data, K-MoCA: Korean version of Montreal cognitive assessment, SD: standard deviation, YearsEducation: years of education, spm: steps per minute, RT_EC: maintenance time of tandem Romberg test when eyes are closed, RT_EO: maintenance time of tandem Romberg test when eyes are opened, VA_un_avg: average of uncorrected visual acuity, BCVA: average of corrected visual acuity, dBHL: decibels hearing level, PTA_B: better results of PTA, either of the two ears at 500, 1000, and 2000 Hz, PTA468_B: better results of PTA, either of the two ears at 4000, 6000, and 8000 Hz, PTA125_B: better results of PTA, either of the two ears at 125, 250, and 500 Hz, SRT_B: better results of SRT, either of the two ears.

highest in NC, followed by N-MIS and L-MIS. Balance function, assessed through RT_EC and RT_EO, showed that NC had the best balance, while L-MIS exhibited the lowest ability. In the case of auditory function, except for PTA468_B, the auditory function variables showed lower threshold values in the order of NC, N-MIS, and L-MIS, indicating a higher hearing ability in NC and a lower hearing ability in L-MIS.

3.2 Machine learning model performance

The models were trained on a subset of variables selected using the SelectKBest algorithm among those listed in Table 2. Figure 2 shows the ROC curves of the classifiers' performances. As shown in Fig. 2, the AUC value for each group was above 0.85 for all four classification models. This indicates the model's excellent capability to differentiate between cognitive decline subtypes.

We evaluated the model's effectiveness by analyzing AUC, accuracy, specificity, and sensitivity and reported our results in Table 3. Among the models tested, the RF model demonstrated the best overall performance.

First, the GB model demonstrated AUC values of 0.926 for L-MIS, 0.932 for N-MIS, and 0.936 for NC, indicating excellent overall discrimination performance. The model's accuracy

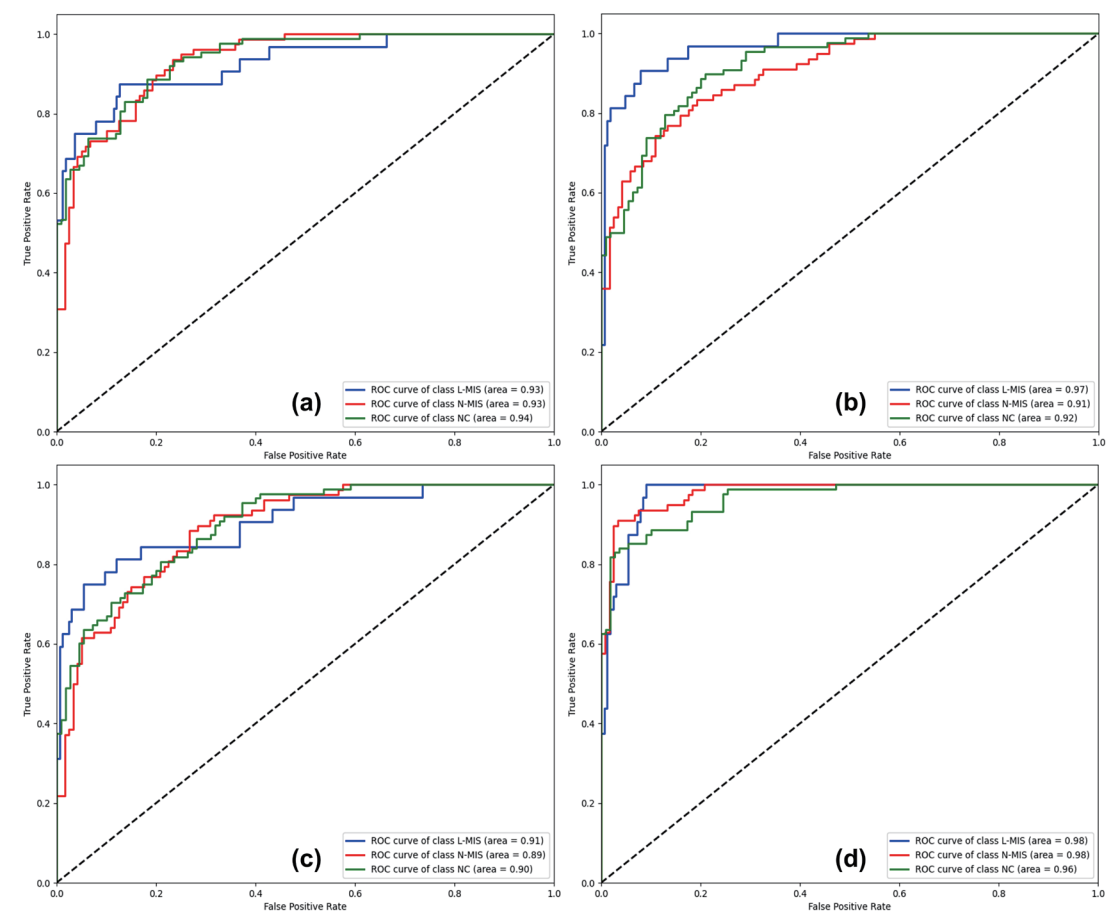


Fig. 2. (Color online) ROC curve of machine learning models: (a) GB, (b) HGB, (c) XGB, and (d) RF.

Table 3
Ensemble learning model performance.

	Group	AUC	Accuracy	Specificity	Sensitivity
GB	L-MIS	0.926	0.748	1.00	0.281
	N-MIS	0.932		0.808	0.769
	NC	0.936		0.755	0.898
HGB	L-MIS	0.969	0.748	0.993	0.312
	N-MIS	0.906		0.817	0.744
	NC	0.921		0.909	0.818
XGB	L-MIS	0.906	0.707	1.00	0.312
	N-MIS	0.892		0.775	0.718
	NC	0.899		0.718	0.841
RF	L-MIS	0.978	0.833	0.988	0.469
	N-MIS	0.981		0.891	0.872
	NC	0.965		0.835	0.932

L-MIS: lower-memory index score, N-MIS: normal-memory index score, NC: normal cognitive, AUC: area under the curve, GB: gradient boosting, HGB: histogram-based gradient boosting, XGB: XGBoost, RF: random forest.

was 0.748, meaning that it correctly classified approximately 75% of the 198 study participants. Specificity values ranged from 0.755 to 1.00. Sensitivity was determined to be 0.281 for L-MIS, the lowest, and 0.898 for NC, the highest.

Second, the HGB model demonstrated excellent classification performance, similarly to the GB model, with AUC values of 0.969 for L-MIS, 0.906 for N-MIS, and 0.921 for NC. The overall accuracy of the HGB model was 0.748, identical to that of the GB model. Specificity was the highest for L-MIS at 0.909 and the lowest for N-MIS at 0.818.

Third, the XGB model demonstrated a slightly lower overall classification performance than the other models, with AUC values of 0.906 for L-MIS, 0.892 for N-MIS, and 0.899 for NC. The overall accuracy of this model was the lowest at 0.707. However, the sensitivity values ranged from 0.312 to 0.841, similar to those of the previous two models. Notably, the specificity of L-MIS in the XGB model was 1.00.

Finally, the RF model demonstrated the best performance, achieving the highest values for AUC, accuracy, sensitivity, and specificity. The AUC values were 0.978 for L-MIS, 0.981 for N-MIS, and 0.965 for NC. The overall accuracy of the RF model was 0.833, meaning that approximately 83% of the study participants were accurately classified. Specificity values were high across all groups: 0.988 for L-MIS, 0.891 for N-MIS, and 0.835 for NC. Additionally, the RF model achieved the highest sensitivity values, with 0.469 for L-MIS, 0.872 for N-MIS, and 0.932 for NC.

4. Discussion

In this study, we demonstrated the substantial utility of motor and sensory function variables in classifying cognitive decline subtypes using machine learning models. In comparison with other studies that predominantly utilize neuropsychological assessments, neuroimaging techniques, and relevant biomarkers for cognitive subtype classification, our approach offers a noninvasive alternative with high diagnostic accuracy.

The RF, GB, XGB, and HGB models were selected for this study because they can handle high-dimensional, small, and imbalanced datasets,^(37,38) which is important for separating different types of cognitive decline. As mentioned in Sect. 2.5.3, RF and GB combine several weak learners to improve predictive performance.⁽³⁷⁾ RF can be used to prevent overfitting through averaging,⁽³⁹⁾ and GB focuses on minimizing bias by sequentially modifying model errors.⁽³⁷⁾ Our results showed that these models are effective and appropriate for our dataset, with RF and GB demonstrating excellent AUC values. Additionally, XGB and HGB provided other advantages. XGB's regularization and scalability help with generalization and accelerate convergence,⁽³⁷⁾ whereas HGB's histogram-based binning method decreases computational costs.⁽⁴⁴⁾ In our study, XGB and HGB showed excellent AUC values and had a better runtime than GB.

The RF model achieved the highest overall performance, with an accuracy of 83.3% and AUC values of 0.978 for L-MIS, 0.981 for N-MIS, and 0.965 for NC. This performance is comparable to, or slightly exceeds, that of other recent studies. For example, Kim *et al.* reported AUC values of 0.947 for aMCI and 0.890 for naMCI when classifying SCD, naMCI, aMCI, and

AD using EEG data.⁽⁴⁵⁾ Liu *et al.* reported a classification accuracy of 72% when distinguishing between aMCI and naMCI using brain function network data.⁽⁴⁶⁾ Similarly, Guan *et al.* reported an accuracy range of 70–80% when classifying NC, aMCI, and naMCI using MRI-based biomarker data.⁽⁴⁷⁾ These methods often require highly specialized equipment and are frequently inaccessible in routine clinical settings, particularly in resource-limited environments.⁽⁴⁸⁾

The AUC value for each group was nearly 0.9 or higher, and the accuracy across all models exceeded 0.7, confirming the strong classification performance of the machine learning models. The N-MIS group's classification sensitivity was lowest in XGB at 0.718 and highest in RF at 0.872. However, when investigating the sensitivity and specificity, the classification sensitivity of the L-MIS group was observed to be 0.281 in GB, 0.312 in HGB and XGB, and 0.469 in RF, indicating lower than optimal performance. Conversely, the specificity exceeded 0.75 for both the L-MIS and N-MIS groups, showing a low false positive rate. The variables used showed more efficacy in identifying N-MIS cases than in identifying L-MIS cases.

The results of this study suggest that gait, balance, and sensory function testing may play a crucial role in the early diagnosis of cognitive decline subtypes, particularly naMCI. Diagnosing naMCI is more challenging than diagnosing aMCI (which can be confirmed via PET or CSF analysis) owing to the presence of amyloid plaques as biomarkers.⁽⁴⁹⁾ In contrast, naMCI lacks such biomarkers, making it more difficult to identify. Moreover, cognitive decline in naMCI is caused by various non-memory-related factors, resulting in diverse clinical symptoms and complicating accurate diagnosis.⁽⁵⁰⁾ While aMCI accounts for 50–70% of MCI cases, naMCI comprises 30–50%,⁽⁵¹⁾ leading to relatively fewer studies on the latter. Therefore, the findings of this study make it easier to find people who are at risk of cognitive decline in areas other than memory. It is also an important tool for early detection.

Gait parameters such as cadence and velocity, which have been shown to differ between individuals with naMCI and aMCI,⁽⁵²⁾ can be easily collected through smartphone sensors or wearable devices.^(53,54) The tandem Romberg test, which requires no specialized equipment, can also be conveniently integrated into routine clinical settings, such as during medical check-ups. As balance function is affected by the autonomic nervous system, the tandem Romberg test may reveal distinct dysfunctions in aMCI, where delayed autonomic responses are more commonly observed than in naMCI.⁽⁵⁵⁾ Similarly, PTA and speech reception threshold, commonly used in routine hearing evaluations and hearing aid fittings, can provide valuable insights, as hearing loss is often linked to memory impairment, aiding in the differentiation between aMCI and naMCI.⁽⁵⁶⁾ These variables are highly useful for the early classification of cognitive decline subtypes.

This study has a couple of limitations. First, despite the promising classification performance of the machine learning model, the sensitivity for the L-MIS group was relatively low, likely due to the small sample size of this group ($n = 32$). The small number of samples may have reduced the model's ability to detect memory impairment patterns in the data. Second, this study included only male participants in good health, mostly younger than 80; therefore, the developed model is applicable to a specific sample of the population. Larger, more diverse datasets would ensure the model's generalizability across various populations; however, obtaining such datasets can be challenging. Future studies should aim to increase the sample size, particularly for small

subgroups such as L-MIS, and to include participants from various populations, which would enable a general, more accurate, and earlier detection of memory-related cognitive decline.

5. Conclusions

In this study, we explored the potential of using motor and sensory parameters to classify subtypes of cognitive decline. Our findings confirmed the applicability of the proposed approach. The best-performing machine learning model achieved an accuracy exceeding 80%, with AUC values above 0.95 for all subgroups. Although the sensitivity for L-MIS was relatively low, the sensitivity for N-MIS was good, demonstrating that motor and sensory variables effectively detect cognitive decline in non-memory domains. Applying these variables in clinical practice can enhance the early detection of naMCI, which is often difficult to diagnose, and support timely intervention to prevent progression to Dementia and any debilitating symptoms.

Acknowledgments

This work was supported by the National Research Foundation of Korea (NRF) grants funded by the Korean government (MSIT) (RS-2022-NR070417) and by the Basic Science Research Program through the National Research Foundation of Korea (NRF) funded by the Ministry of Education (RS-2022-NR074923). The funders had no role in the study design, data collection and analysis, decision to publish, or preparation of the manuscript.

References

- 1 W. Bai, P. Chen, H. Cai, Q. Zhang, Z. Su, T. Cheung, T. Jackson, S. Sha, and Y. T. Xiang: Age Ageing **51** (2022) 1. <https://doi.org/10.1093/ageing/afac173>
- 2 R. C. Petersen, G. E. Smith, S. C. Waring, R. J. Ivnik, E. G. Tangalos, and E. Kokmen: Arch. Neurol. **56** (1999) 303. <https://doi.org/10.1001/archneur.56.3.303>
- 3 R. C. Petersen, O. Lopez, M. J. Armstrong, T. S. D. Getchius, M. Ganguli, and D. Gloss: Neurology **90** (2018) 126. <https://doi.org/10.1212/WNL.0000000000004826>
- 4 K. M. Langa and D. A. Levine: JAMA **312** (2014) 2551. <https://doi.org/10.1001/jama.2014.13806>
- 5 M. Malek-Ahmadi: Alzheimer Dis. Assoc. Disord. **30** (2016) 324. <https://doi.org/10.1097/WAD.0000000000000145>
- 6 K. Yaffe, R. C. Petersen, K. Lindquist, J. Kramer, and B. Miller: Dementia Geriatr. Cogn. Disord. **22** (2006) 312. <https://doi.org/10.1159/000095427>
- 7 R. C. Petersen, P. Aisen, B. F. Boeve, Y. E. Geda, R. J. Ivnik, D. S. Knopman, M. Mielke, V. S. Pankratz, R. Roberts, W. A. Rocca, S. Weigand, M. Weiner, H. Wiste, and C. R. Jack Jr.: Ann. Neurol. **74** (2013) 199. <https://doi.org/10.1002/ana.23931>
- 8 M. Iraniparast, Y. Shi, Y. Wu, L. Zeng, C. J. Maxwell, R. J. Kryscio, P. D. St. John, K. S. SantaCruz, and S. L. Tyas: Neurology **98** (2022) e1114. <https://doi.org/10.1212/WNL.0000000000200051>
- 9 J. Chen, Z. Zhang, and S. Li: Neurosci. Bull. **31** (2015) 128. <https://doi.org/10.1007/s12264-014-1490-8>
- 10 B. Winblad, K. Palmer, M. Kivipelto, V. Jelic, L. Fratiglioni, L.-O. Wahlund, A. Nordberg, L. Bäckman, M. Albert, O. Almkvist, H. Arai, H. Basun, K. Blennow, M. De Leon, C. DeCarli, T. Erkinjuntti, E. Giacobini, C. Graff, J. Hardy, C. Jack, A. Jorm, K. Ritchie, C. Van Duijn, P. Visser, and R. C. Petersen: J. Int. Med. **256** (2004) 240. <https://doi.org/10.1111/j.1365-2796.2004.01380.x>
- 11 M. Liu, D. Zhang, and D. Shen: Hum. Brain Mapp. **35** (2013) 1305. <https://doi.org/10.1002/hbm.22254>
- 12 D. S. Knopman, R. O. Roberts, Y. E. Geda, B. F. Boeve, V. S. Pankratz, R. H. Cha, E. G. Tangalos, R. J. Ivnik, and R. C. Petersen: Arch. Neurol. **66** (2009) 614. <https://doi.org/10.1001/archneurol.2009.30>
- 13 R. C. Petersen, R. Doody, A. Kurz, R. C. Mohs, J. C. Morris, P. V. Rabins, K. Ritchie, M. Rossor, L. Thal, and B. Winblad: Arch. Neurol. **58** (2001) 1985. <https://doi.org/10.1001/archneur.58.12.1985>

- 14 P. J. Snyder, Y. Y. Lim, R. Schindler, B. R. Ott, S. Salloway, L. Daiello, C. Getter, C. M. Gordon, and P. Maruff: *Alzheimers Dement.* **10** (2014) 262. <https://doi.org/10.1016/j.jalz.2014.01.009>
- 15 K. J. Bangen, A. L. Clark, M. Werhane, E. C. Edmonds, D. A. Nation, N. Evangelista, D. J. Libon, M. W. Bondi, L. Delano-Wood, and Alzheimer's Disease Neuroimaging Initiative: *J. Alzheimers Dis.* **52** (2016) 849. <https://doi.org/10.3233/JAD-150900>
- 16 M. W. Albers, G. C. Gilmore, J. Kaye, C. Murphy, A. Wingfield, D. A. Bennett, A. L. Boxer, A. S. Buchman, K. J. Cruickshanks, D. P. Devanand, C. J. Duffy, C. M. Gall, G. A. Gates, A. C. Granholm, T. Hensch, R. Holtzer, B. T. Hyman, F. R. Lin, A. C. McKee, J. C. Morris, R. C. Petersen, L. C. Silbert, R. G. Struble, J. Q. Trojanowski, J. Verghese, D. A. Wilson, S. Xu, and L. I. Zhang: *Alzheimers Dement.* **11** (2015) 70. <https://doi.org/10.1016/j.jalz.2014.04.514>
- 17 M. Montero-Odasso, A. Oteng-Amoako, M. Speechley, K. Gopaul, O. Beauchet, C. Annweiler, and S. W. Muir-Hunter: *J. Gerontol. A. Biol. Sci. Med. Sci.* **69** (2014) 1415. <https://doi.org/10.1093/gerona/glu155>
- 18 J. M. Hausdorff, D. A. Rios, and H. K. Edelberg: *Arch. Phys. Med. Rehabil.* **82** (2001) 1050. <https://doi.org/10.1053/apmr.2001.24893>
- 19 L. Pisella: *Ann. Phys. Rehabil. Med.* **60** (2017) 141. <https://doi.org/10.1016/j.rehab.2016.01.002>
- 20 M. M. Machulda, M. L. Senjem, S. D. Weigand, G. E. Smith, R. J. Ivnik, B. F. Boeve, D. S. Knopman, R. C. Petersen, and C. R. Jack: *J. Int. Neuropsychol. Soc.* **15** (2009) 372. <https://doi.org/10.1017/S1355617709090523>
- 21 R. Bougeard and C. Fischer: *Epileptic Disord.* **4** (2002) S29. <https://doi.org/10.1684/j.1950-6945.2002.tb00516.x>
- 22 P. Calvini, A. Chincarini, G. Gemme, M. A. Penco, S. Squarcia, F. Nobili, G. Rodriguez, R. Bellotti, E. Catanzariti, P. Cerello, I. De Mitri, and M. E. Fantacci: *MAGIC-5 Collaboration; Alzheimer's Disease Neuroimaging Initiative: Med. Phys.* **36** (2009) 3737. <https://doi.org/10.1118/1.3171686>
- 23 Z. Wang, J. Wang, J. Guo, A. Dove, K. Arfanakis, X. Qi, D. Bennett, and W. Xu: *Neurology* **101** (2023) e1718. <https://doi.org/10.1212/WNL.0000000000207745>
- 24 E. Magosso and M. Ursino: *J. Integr. Neurosci.* **22** (2022) 3. <https://doi.org/10.31083/j.jin.2201003>
- 25 Z. S. Nasreddine, N. A. Phillips, V. Bédirian, S. Charbonneau, V. Whitehead, I. Collin, J. L. Cummings, and H. Chertkow: *J. Am. Geriatr. Soc.* **53** (2005) 695. <https://doi.org/10.1111/j.1532-5415.2005.53221.x>
- 26 A. Kaur, S. D. Edland, and G. M. Peavy: *Alzheimer Dis. Assoc. Disord.* **32** (2018) 120. <https://doi.org/10.1097/WAD.0000000000000238>
- 27 J. Verghese, C. Wang, R. B. Lipton, R. Holtzer, and X. Xue: *J. Neurol. Neurosurg. Psychiatry* **78** (2007) 929. <https://doi.org/10.1136/jnnp.2006.106914>
- 28 A. M. V. Wennberg, R. Savica, C. E. Hagen, R. O. Roberts, D. S. Knopman, J. H. Hollman, P. Vemuri, C. R. Jack Jr, R. C. Petersen, and M. M. Mielke: *J. Am. Geriatr. Soc.* **65** (2017) 792. <https://doi.org/10.1111/jgs.14670>
- 29 M. Fatima and M. Pasha: *J. Intell. Learn. Syst. Appl.* **9** (2017) 1. <https://doi.org/10.4236/jilsa.2017.91001>
- 30 N. Olabi, A. Yilmaz, and Z. Aslan: *EURAS J. Health* **2** (2020) 129. https://doi.org/10.17932/ejoh.2020.022/ejoh_v02i2004
- 31 Q. Meng: *Appl. Comput. Eng.* **33** (2024) 207. <https://doi.org/10.54254/2755-2721/33/20230268>
- 32 S. Bansal: *Biomed. Stat. Inf.* **6** (2021) 84. <https://doi.org/10.11648/j.bsi.20210604.13>
- 33 J. D. Mello-Román, J. C. M. Román, S. Gómez-Guerrero, and M. García-Torres: *Comput. Math. Methods Med.* **2019** (2019) 1. <https://doi.org/10.1155/2019/7307803>
- 34 C. Wang and Y. Huang: *Expert Syst. Appl.* **36** (2009) 5900. <https://doi.org/10.1016/j.eswa.2008.07.026>
- 35 F. Pedregosa, G. Varoquaux, A. Gramfort, V. Michel, B. Thirion, O. Grisel, M. Blondel, P. Prettenhofer, R. Weiss, V. Dubourg, J. Vanderplas, A. Passos, D. Cournapeau, M. Brucher, M. Perrot and É. Duchesnay: *J. Mach. Learn. Res.* **12** (2011) 2825. <https://doi.org/10.48550/arXiv.1201.0490>
- 36 J. F. Hair Jr, W. C. Black, B. J. Babin, and R. E. Anderson: *Multivariate Data Analysis* (Cengage Learning, United Kingdom, 2018) 8th ed., Chap. 5.
- 37 O. Sagi and L. Rokach: *Wiley Interdiscip. Rev. Data Min. Knowl. Discov.* **8** (2018) e1249. <https://doi.org/10.1002/widm.1249>
- 38 A. Doganer: *Int. J. Big Data Anal. Healthcare* **6** (2021) 15. <https://doi.org/10.4018/IJBDAH.20210701.oa2>
- 39 L. Breiman: *Mach. Learn.* **24** (1996) 123. <https://doi.org/10.1023/A:1018054314350>
- 40 C. Bentéjac, A. Csörgő, and G. Martínez-Muñoz: *Artif. Intell. Rev.* **54** (2021) 1937. <https://doi.org/10.1007/s10462-020-09896-5>
- 41 T. Hastie, R. Tibshirani, J. H. Friedman, J. H. Friedman: *The Elements of Statistical Learning: Data Mining, Inference, and Prediction* (Springer, New York, 2009) 2nd ed., pp. 1–758.
- 42 J. Y. Verbakel, E. W. Steyerberg, H. Uno, B. De Cock, L. Wynants, G. S. Collins, and B. Van Calster: *J. Clin. Epidemiol.* **126** (2020) 207. <https://doi.org/10.1016/j.jclinepi.2020.06.031>
- 43 J. A. Hanley and B. J. McNeil: *Radiology* **143** (1982) 29. <https://doi.org/10.1148/radiology.143.1.7063747>

- 44 G. Ke, Q. Meng, T. Finley, T. Wang, W. Chen, W. Ma, Q. Ye, and T.-Y. Liu: Proc. 31st Conf. Neural Information Processing Systems (NeurIPS) (Microsoft Research, 2017) 3149–3157.
- 45 S. K. Kim, H. Kim, S. H. Kim, J. B. Kim, and L. Kim: Sci. Rep. **14** (2024) 5252. <https://doi.org/10.1038/s41598-024-55656-8>
- 46 M. Liu, L. Cui, Z. Zhao, S. Ren, L. Huang, Y. Guan, Q. Guo, F. Xie, Q. Huang, and D. Shen: Cereb. Cortex. **33** (2023) 11486. <https://doi.org/10.1093/cercor/bhad381>
- 47 H. Guan, T. Liu, J. Jiang, D. Tao, J. Zhang, H. Niu, W. Zhu, Y. Wang, J. Cheng, N. Kochan, H. Brodaty, P. Sachdev, and W. Wen: Front. Aging Neurosci. **9** (2017) 309. <https://doi.org/10.3389/fnagi.2017.00309>
- 48 H. C. McLane, A. L. Berkowitz, B. N. Patenaude, E. D. McKenzie, E. Wolper, S. Wahlster, G. Fink, and F. J. Mateen: Neurology **85** (2015) 1614. <https://doi.org/10.1212/WNL.0000000000002090>
- 49 Y. Qu, Y. H. Ma, Y. Y. Huang, Y. N. Ou, X. N. Shen, S. D. Chen, Q. Dong, L. Tan, and J. T. Yu: Neurosci. Biobehav. Rev. **128** (2021) 479. <https://doi.org/10.1016/j.neubiorev.2021.07.007>
- 50 R. C. Petersen: J. Intern. Med. **256** (2004) 183. <https://doi.org/10.1111/j.1365-2796.2004.01388.x>
- 51 G. Zuliani, M. Polastri, T. Romagnoli, L. Marabini, D. Seripa, C. Cervellati, A. Zurlo, A. Passaro, and G. Brombo: Aging Clin. Exp. Res. **33** (2020) 1895. <https://doi.org/10.1007/s40520-020-01697-8>
- 52 J. Verghese, M. Robbins, R. Holtzer, M. Zimmerman, C. Wang, X. Xue, and R. B. Lipton: J. Am. Geriatr. Soc. **56** (2008) 1244. <https://doi.org/10.1111/j.1532-5415.2008.01758.x>
- 53 J. R. Mahoney, H. M. Blumen, P. De Sanctis, R. Fleysher, C. Frankini, A. Hoang, M. J. Hoptman, R. Jin, M. Lipton, V. Nunez, L. Twizer, N. Uy, A. Valdivia, T. Verghese, C. Wang, E. F. Weiss, J. Zwerling, and J. Verghese: Front. Aging Neurosci. **15** (2023) 1125114. <https://doi.org/10.3389/fnagi.2023.1125114>
- 54 L. C. Benson, C. A. Clermont, E. Bošnjak, and R. Ferber: Gait Posture. **63** (2018) 124. <https://doi.org/10.1016/j.gaitpost.2018.04.047>
- 55 P. Nicolini, D. Mari, C. Abbate, S. Inglese, L. Bertagnoli, E. Tomasini, P. Rossi, and F. Lombardi: Sci. Rep. **10** (2020) 68131. <https://doi.org/10.1038/s41598-020-68131-x>
- 56 P. Croll, E. Vinke, N. Armstrong, S. Licher, M. Vernooij, R. De Jong, A. Goedegebure, and M. A. Ikram: J. Neurol. **268** (2020) 860. <https://doi.org/10.1007/s00415-020-10208-8>

About the Authors



Sinyoung Lee received her B.S. and M.S degrees from Jeonbuk National University, Republic of Korea, in 2022 and 2024, respectively. She is currently in the process of obtaining her Ph.D. degree at Jeonbuk National University. Her research interests are in healthcare systems, sensory processing, and cognition function in the elderly.



Kiyoun Kwak received his B.S., M.S., and Ph.D. degrees from Jeonbuk National University, Republic of Korea, in 2009, 2011, and 2018, respectively. He is currently a postdoctoral researcher at the Division of Biomedical Engineering, Jeonbuk National University. His major research interests are in neuro-musculoskeletal biomechanics, sensory–motor integration, rehabilitation engineering, and cognition function in the elderly.



Emilija Kostic received her B.S. degree from the University of Belgrade, Serbia, in 2018, and her M.S. and Ph.D. degrees from Jeonbuk National University, Republic of Korea, in 2021, and 2025, respectively. Her major research interests are in machine learning utilization in healthcare, sensory processing, rehabilitation engineering, and elderly cognition.



Dongwook Kim received his Ph.D. degree in biomedical engineering from Hokkaido University, Sapporo, Japan, in 1995. He is now a professor at the Division of Biomedical Engineering, Jeonbuk National University, Republic of Korea. Also, he was the president of the Korean Society of Medical and Biological Engineering from January to December 2021. His current research interests include biomedical engineering, rehabilitation engineering, sensory–motor integration, diagnosis, and healthcare systems.